frontiers in Physics

ORIGINAL RESEARCH
published: 10 January 2020
doi: 10.3389/fphy.2019.00216

Low Threshold, High Efficiency Passively Mode-Locked Picosecond Tm,Ho:$LiLuF_4$ Laser

Weijun Ling[1]*, *Tao Xia*[1], *Rui Sun*[1,2], *Chen Chen*[1,2], *Qiang Xu*[1,2] *and Yani Zhang*[2,3]*

[1] Institute of Laser Technology, Tianshui Normal University, Tianshui, China, [2] School of Physics and Optoelectronics Technology, Baoji University of Arts and Science, Baoji, China, [3] School of Arts and Sciences, Shaanxi University of Science and Technology, Xi'an, China

We experimentally demonstrated a passively mode-locked picosecond Tm,Ho:$LiLuF_4$ laser with low threshold and high efficiency. The stable continuous-wave (CW) mode-locked operation with 12 ps pulse width is obtained by using a five-mirror cavity structure and semiconductor saturable absorber mirrors (SESAMs). The results indicate that the laser offers a mode-locked threshold power of 1.03 W and maximum mode-locked output power of 350 mW. The repetition rate of mode-locked pulse sequence is 98.04 MHz, corresponding a maximum single pulse energy of 3.51 nJ.

Keywords: Tm,Ho:LLF laser, resonant cavity, low threshold, continuous-wave mode locking, semiconductor saturable absorber mirrors
OCIS codes: 140.3070, 140.3580, 140.3430, 140.4050

OPEN ACCESS

Edited by:
Xueming Liu,
Zhejiang University, China

Reviewed by:
Jiangfeng Zhu,
Xidian University, China
Guoqiang Xie,
Shanghai Jiao Tong University, China

***Correspondence:**
Weijun Ling
wjlingts@sina.com
Yani Zhang
yanizhang1@163.com

Specialty section:
This article was submitted to Optics and Photonics, a section of the journal Frontiers in Physics

Received: *23 October 2019*
Accepted: *27 November 2019*
Published: *10 January 2020*

Citation:
Ling W, Xia T, Sun R, Chen C, Xu Q and Zhang Y (2020) Low Threshold, High Efficiency Passively Mode-Locked Picosecond Tm,Ho:$LiLuF_4$ Laser. Front. Phys. 7:216. doi: 10.3389/fphy.2019.00216

INTRODUCTION

In recent years, 2 μm ultrashort-pulsed lasers based on doped Tm^{3+} or co-doped Tm^{3+} & Ho^{3+} are one of the frontier research contents of ultrafast laser technology. The emission peak of a Tm^{3+} doped laser is located near the strong absorption peak of water, at 1.93 μm, so it has the characteristics of a low penetration depth and has important applications in ophthalmic laser surgery, tumorectomy [1, 2]. Moreover, the laser has excellent atmospheric permeability and will play an important role in military and space communication fields. The laser spectrum is also located in the "fingerprint" region of the reaction molecule's absorption characteristics, so it has important application value in the field of accurate time-resolved molecular spectroscopy [3]. As a pump source, it has an important application in 3–5 μm mid-infrared band generation, mid-infrared supercontinuum generation and THz band pulse generation [4]. However, realizing a mode-locked operation is one of the technical difficulties it faces due to Q-switching, caused by water molecular absorption and gain medium spectral modulation.

Compared with other matrix materials, Tm,Ho:$LiLuF_4$ (Tm,Ho:LLF) is an excellent laser crystal with relatively low phonon energy, lower laser threshold and small up-conversion loss [5]. In 2010, Peng et al. reported a CW Tm,Ho:LLF laser with a central wavelength of 2.05 um and an output power of 50 mW [6]. In 2013, Zhang et al. used Cr2+:ZnS as a saturated absorber to realize Q-switching and Q-switching mode-locking operation of Tm,Ho:LLF laser [7, 8]. It was not until 2018 that Ling et al. realized the Q-switched mode locking operation of Tm:LLF laser [9].

It is well known that the passively mode-locked operation of a 2 μm band can be obtained by periodically controlling the loss of the resonator with the saturable absorber (SA). Based on characteristics of tunable material non-linear absorption coefficient, short relaxation time and recovery time and low optical loss, more and more optical materials have been applied in the field of lasers, such as SESAM, graphene, graphene oxide, topological insulators (TI), single-walled carbon nanotubes (SWCNT),

etc. [10–12]. The SESAM is a major mode-locked element with mature commercial performance and stable mode locking characteristics. Picosecond or femtosecond mode-locking operation has been realized in crystals Tm: CLNGG [13], Tm,Ho:NaY $(WO_4)_2$ [14], Tm: Sc_2O_3 [15], Tm:$CaGdAlO_4$ [16], Tm: $CaYAlO_4$ [17], Tm: Lu_2O_3 ceramics [18], Tm,Ho:CNGG [19], and Tm,Ho:CLNGG [20]. Ma et al. Comprehensively analyzed the mode-locked characteristics of this kind of lasers [21].

In this paper, we demonstrate a low threshold and high efficiency mode-locked Tm,Ho:LLF laser by using a five-mirror cavity structure. The results show that the crystal achieves the current highest efficiency of 53.6% under CW operation; the maximum mode-locked output power is 350 mW at 1,895 nm, and the typical pulse width is 12 ps. Moreover, the minimum CW threshold power is 59 mW, and the mode-locked threshold power is 1.03 W. Because the output power of Ti: sapphire laser is positively correlated with the cost, the low threshold design of the laser can not only effectively reduce the cost, but also provide a new idea for the application of laser.

EXPERIMENTAL SETUP

The experimental setup of CW mode-locked Tm,Ho:LLF laser is shown in **Figure 1**. The five-mirror cavity system mainly includes a typical X- type four-mirror folded cavity and focused concave mirror. The resonator has an oscillating spot of tens of microns, which greatly reduces the laser threshold. The laser efficiency can be improved easily by optimizing the matching of pumping and oscillating spots. The pump source is a self-made Ti-doped sapphire laser. **Figure 2** shows the absorption spectrum of Tm,Ho:LLF. From **Figure 2**, it is observed that the central wavelength of the strongest absorption peak of Tm,Ho:LLF crystal is 780.5 nm, and the half-width is 1 nm. Tm,Ho:LLF crystal is cut at the angle of Brewster. The two end faces are polished. The doped concentrations of Tm^{3+} and Ho^{3+} are 5 and 0.5%, respectively. The size of the crystal is 3 × 3 × 8 mm. The laser crystal is wrapped in indium foil and clamped in a copper radiator. The copper clamp is cooled by 8°C constant temperature circulating water cooling system. The focal length of the focusing lens L_2 is 120 mm. The focal length of the pumping concave mirror M_9 is 100 mm, and the focal length of the M_{10} is 75 mm, which has a transmittance of more than 95% at 770–1,050 nm and reflectance of more than 99.9% at 1,800–2,075 nm. The transmittance of output coupling (OC) mirror M_{11} is 3%. The radius of concave mirror M_{12} is 100 mm. M_{13} is a plane high-reflectivity mirror with a reflectivity of more than 99.9% at 1,800–2,075 nm. The SESAM is GaAs-SESAM with a modulation depth of 1.2% and a relaxation time of 10 ps (BATOP, Germany). The waist radius of SESAM is about 180 μm, and the energy flux is 117 $\mu J/cm^2$, which is larger than SESAM saturated flux of 70 μJ/cm. P_1 and P_2 are CaF_2 prism pairs with a distance of 35 cm, which mainly compensate for the second-order dispersion produced by intracavity crystals and self-phase modulation.

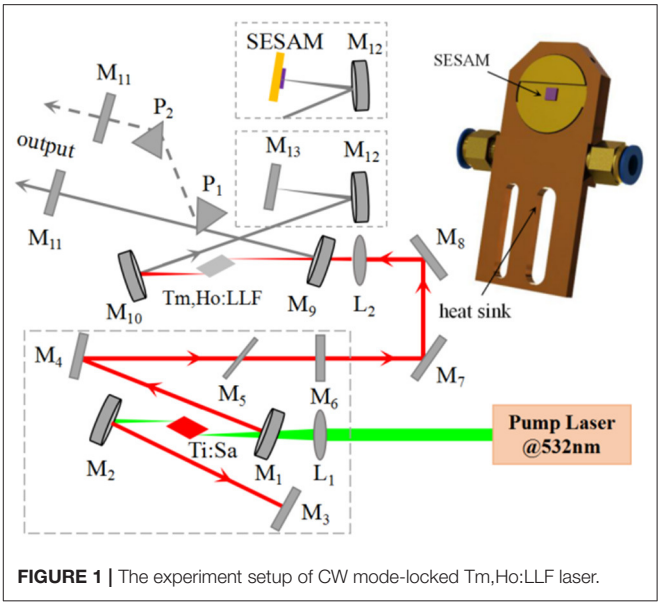

FIGURE 1 | The experiment setup of CW mode-locked Tm,Ho:LLF laser.

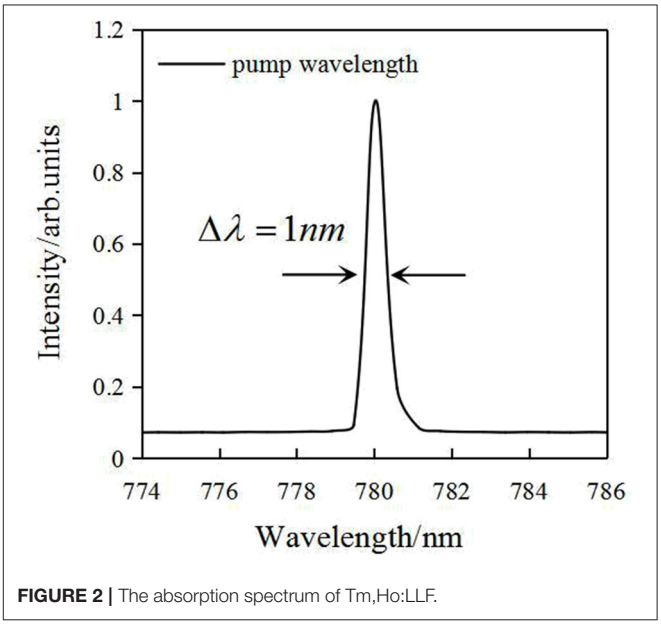

FIGURE 2 | The absorption spectrum of Tm,Ho:LLF.

EXPERIMENTAL RESULTS AND DISCUSSION

The folding mirror is composed of M_{10} and M_9. The radius of curvature of M_9 is 100 mm. In order to achieve high efficiency and low threshold operation by mode matching of pumping light and oscillating light, the curvature radius of the folding mirror M_{10} is 100, 75, and 50 mm, respectively. The corresponding folding cavity is marked as (100, 100), (100, 75), (100, 50). The absorption efficiency of the crystal is shown in **Figure 3A**. It can be seen that the absorption efficiency of the crystal is 35.3% without laser oscillation. After the laser oscillation, the absorption efficiency of the crystal increases due

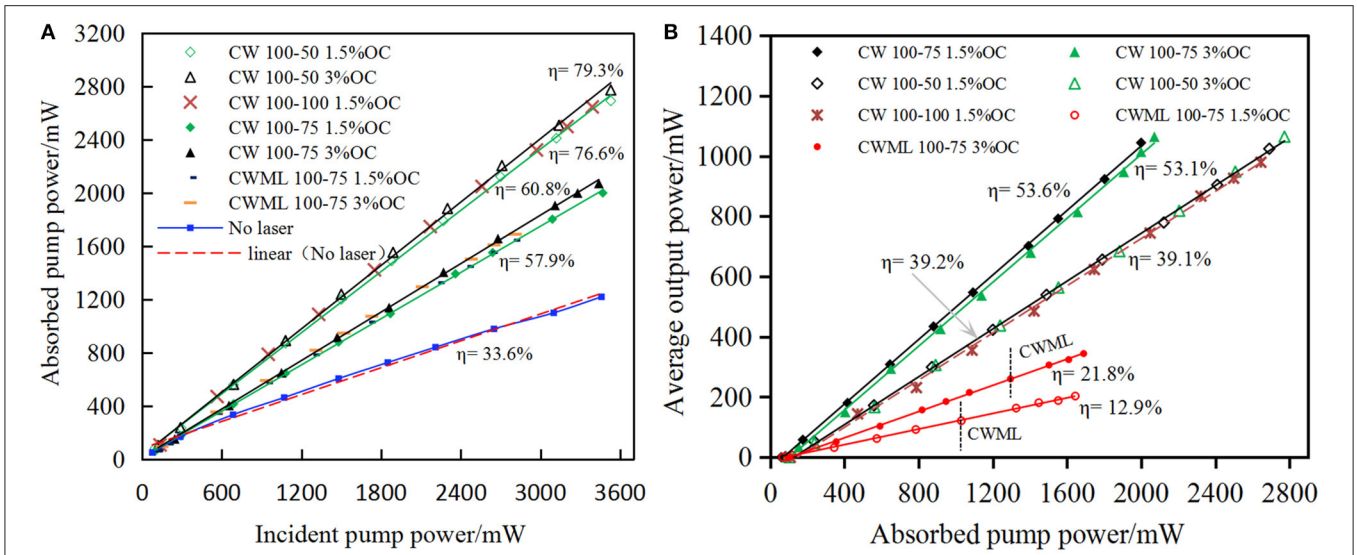

FIGURE 3 | (A) Relation between incident pump power and absorption power. **(B)** Relation between average output power and absorption pump power under CW and mode-locked operation.

TABLE 1 | The continuous wave parameters of different pump mirrors.

M_9 (mm)	M_{10} (mm)	M_{11} OC (%)	threshold power (mW)	Crystal absorption efficiency (%)	Slope efficiency (%)	Output average power (mW)	Optical to optical efficiency (%)
100	100	1.5%	108	77.6%	39.1%	979	28.88%
100	75	1.5%	59	57.9%	53.6%	1,044	30.09%
100	75	3%	88	60.7%	53.1%	1,064	30.93%
100	50	1.5%	81	76.6%	39.2%	1,024	29.01%
100	50	3%	104	79.3%	39.7%	1,064	30.14%

to the consumption of a large number of upper-level particles and varies with the coupling ratio of the output mirror. The transmittance of the output mirror is 1.5 and 3% respectively. When M_{10} is 100 and 50 mm, the absorption efficiency of the crystal is at the highest. When M_{10} is 75 mm, the absorption efficiency of the crystal is between 57.9 and 60.8%. When SESAM and CaF_2 prisms are added into the cavity, M_{10} is chosen as 75 mm, and the absorption efficiency of the crystal is about 59%. It can be seen that the beam waist radius of the oscillating light in the crystal will be determined by the choice of different folding mirrors, which will affect the absorption efficiency of the crystal. At the same pump power, CW and mode-locked operation will not affect the absorption efficiency of the crystal.

As can be seen from **Table 1**, the 1.5% OC and (100, 75) cavity can achieve the operation of low threshold and high efficiency. The CW threshold power is as low as 59 mW, the slope efficiency is up to 53.6%, the maximum output power is 1.04 W, and the corresponding optical-optical conversion efficiency is 30.09%. So (100, 75) cavity is chosen as mode-locked cavity in the experiment. When the M_{13} plane reflector is replaced by SESAM and the CaF_2 prism is inserted into the cavity to compensate dispersion, the laser threshold is increased to 67 mW. When the absorption pump power is >1.03 W, the stable CW mode-locked operation is realized, and the maximum output power is 203 mW, and the slope efficiency is 12.9%. With 3% output mirror, the CW threshold power is 88 mW, and the pump power is gradually increased. When the absorption pump power is >1.3 W, a stable CW mode-locked operation is obtained. The maximum output power is 350 mW and the slope efficiency is 21.8%.

It is found that the difference between the mode-locked threshold power of 1.5% output coupling mirror and that of 3% OC is little; the mode-locking threshold of 1.5% is 1.03 W and that of 3% output coupling mirror is 1.3 W. The main reason for this is that the passive mode-locking is soliton mode-locking [22–24], and the threshold of mode-locking is mainly determined by the energy flux density on the surface of SESAM. So when mode locking is started, the energy flux density on the surface of SESAM for 3% OC and 1.5% OC should be the same, i.e., corresponding to the same cavity power. So theoretically, the output power of 3% OC should be twice that of 1.5% OC. From **Figure 3B**, it can be seen that when mode locking is started, the output power of 3% OC is 260 mw, which is approximately twice the output power 128 mW of 1.5% OC, which is consistent with our theoretical prediction.

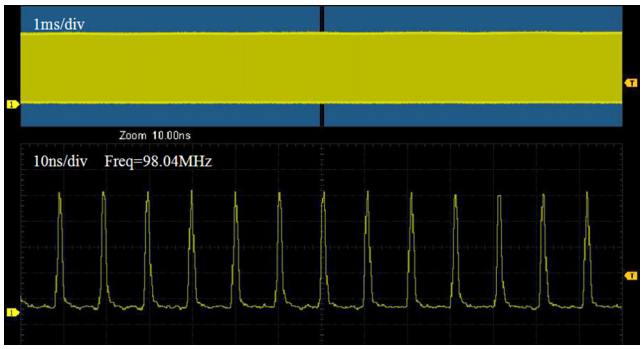

FIGURE 4 | Mode-locked pulse sequence when scanning time was 1 ms and 10 ns, respectively.

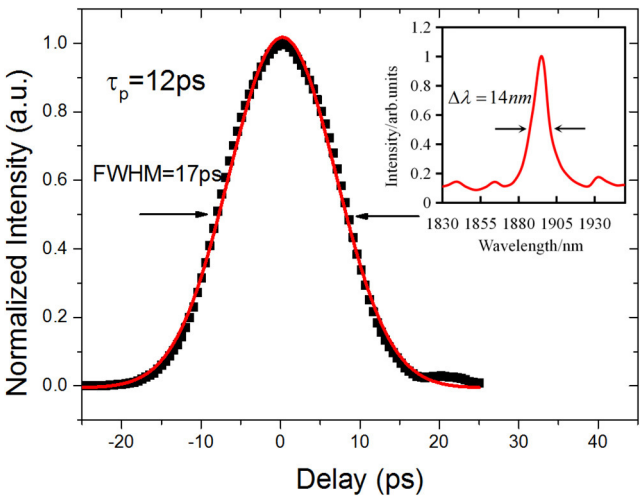

FIGURE 5 | The measured autocorrelation curve with fit (black dots) and mode-locked spectrum (inset).

Because the central wavelength of the mode-locked spectrum is 1,895 nm, which is near the absorption band of water molecules, in order to achieve stable mode-locked operation, we use the dehumidifier to reduce the indoor air relative humidity to about 30%, and the decrease of air humidity can also reduce the cooling temperature of crystal to a lower level without condensation water. In this experiment, the cooling temperature of the crystal is 8°C, which greatly reduces the thermal lens effect of the crystal. Thermal noise generated by heat accumulation on SESAM also affects the stability of mode-locking. Therefore, we designed a water-cooling device for SESAM, which can keep the temperature of SESAM stable at about 8°C. This cooling device improves the stability of mold locking and prolongs the operation time of mold locking.

The detection of CW mode-locked pulse sequence is realized by connecting a 200 MHz digital oscilloscope (RIGOL, DS4024) with a fast photodiode (EOT, ET-5000). **Figure 4** shows a CW mode-locked pulse sequence with repetition rate of 98.04 MHz, which is obtained with scanning time of 1 ms and 10 ns. As shown in the inset of **Figure 5**, the spectrum of the mode-locked pulse is measured by a spectral analyzer (AvaSpec-NIR256-2.5TEC). The central wavelength of the output CW mode-locked pulse is 1,895 nm, and the half-width of the spectrum is 14 nm. The autocorrelation envelope pulse width measured by autocorrelator (APE, pulse check 50) is 17 ps, and the actual pulse width is 12 ps by $sech^2$ function fitting, as shown in **Figure 5**.

CONCLUSION

In summary, the folding mirrors with different curvatures are selected for a comprehensive comparison at CW operation. It is concluded that the laser cavity (100, 75) has the best comprehensive output performance under a 1.5% OC mirror. The laser threshold power is as low as 59 mW, the maximum power is 1.04 W, the slope efficiency is 53.6%, and the optical-optical conversion efficiency is 30.09%. So we choose (100, 75) cavity to study mode-locked operation. Using GaAs-SESAM as a mode-locked starter and self-made water cooling system to eliminate the thermal noise of SESAM, a high efficiency CW mode-locked operation of Tm,Ho:LLF laser is realized. Under 3% OC mirror, the maximum power of 350 mW, the shortest pulse width of 12 ps and the repetition rate of 98.04 MHz are obtained, corresponding to the maximum single pulse energy of 3.51 nJ. In the next step, we will use graphene, SWCNT or other low loss SA to reduce the loss of the whole cavity and achieve shorter mode-locked pulse with reasonable dispersion compensation.

DATA AVAILABILITY STATEMENT

All datasets generated for this study are included in the article/supplementary material.

AUTHOR CONTRIBUTIONS

WL was the author of the experimental scheme and the general director of the project. TX, RS, and CC were graduate students of the research group, who implement the experimental scheme. QX and YZ were the specific guidance for postgraduates during the experiment.

FUNDING

This work was supported by the National Natural Science Foundation of China (Nos. 11774257, 61564008, 11647008, and 11504416), the International Science & Technology Cooperation and Exchanges Project of Shaanxi (No. 2014KW07-01), and the Key Sciences and Technology Project of Baoji City (No. 2015CXNL-1-3).

REFERENCES

1. Wang J, Sramek C, Paulus YM, Lavinsky D, Schuele G, Anderson D, et al. Retinal safety of near-infrared lasers in cataract surgery. *J Biomed Opt.* (2012) **17**:95001. doi: 10.1117/1.JBO.17.9.095001
2. van Leeuwen TG, Jansen ED, Motamedi M, Welch AJ, Borst, C. Excimer laser ablation of soft tissue: a study of the content of rapidly expanding and collapsing bubbles. *IEEE J Quant Electron.* (2002) **30**:1339–45. doi: 10.1109/3.303700
3. Sorokin E, Sorokina IT, Mandon J, Guelachvili G, Picqué N. Sensitive multiplex spectroscopy in the molecular fingerprint 2.4 mum region with a Cr(2+):ZnSe femtosecond laser. *Opt Exp*. (2007) **15**:16540–5. doi: 10.1364/OE.15.016540
4. Koopmann P, Lamrini S, Scholle K, Fuhrberg P, Petermann K, Huber G. Efficient diode-pumped laser operation of $Tm:Lu_2O_3$ around 2 μm. *Opt Lett.* (2011) **36**:948–50. doi: 10.1364/OL.36.000948
5. Qiao L, Yang FG, Wu YH, Ke YG, Xia ZC. Theoretical and experimental researches on Tm and Ho codoped Q-switching laser. *Acta Phys Sin.* (2014) **63**:137–43. doi: 10.7498/aps.63.214205
6. Peng H, Zhang K, Zhang L, Hang Y, Xu J, Tang Y, et al. Spectroscopic properties of Tm,Ho:LiLuF4. *Chin Opt Lett.* (2010) **8**:63–5. doi: 10.3788/COL20100801.0063
7. Zhang X, Yu L, Zhang S, Li L, Zhao J, Cui J. Diode-pumped continuous wave and passively Q-switched Tm,Ho:LLF laser at 2 μm. *Opt Exp*. (2013) **21**:12629–34. doi: 10.1364/OE.21.012629
8. Zhang XL, Zhang S, Xiao NN, Zhao JQ, Li L, Cui JH. Diode-pumped passively Q-switched dual-wavelength c-cut Tm,Ho:LLF laser at 2 μm. *Laser Phys Lett*. (2014) **11**:035801. doi: 10.1088/1612-2011/11/3/035801
9. Ling WJ, Xia T, Dong Z, Liu Q, Lu FP, Wang YG. Passively Q-switched mode-locked Tm,Ho:LLF laser with a WS_2 saturable absorber. *Acta Phys Sin.* (2007) **66**:130–5. doi: 10.7498/aps.66.114207
10. Liu X, Pang M. Revealing the Buildup Dynamics of Harmonic Mode mocking States in Ultrafast Lasers. *Laser Photonics Rev.* (2019) **13**:1800333. doi: 10.1002/lpor.201800333
11. Cho WB, Schmidt A, Yim JH, Choi SY, Lee S, Rotermund F, et al. Passive mode-locking of a Tm-doped bulk laser near 2 microm using a carbon nanotube saturable absorber. *Opt Exp*. (2009) **17**:11007–12. doi: 10.1364/OE.17.011007
12. Liu X. Hysteresis phenomena and multipulse formation of a dissipative system in a passively mode-locked fiber laser. *Phys Rev A*. (2010) **81**:023811. doi: 10.1103/PhysRevA.81.023811
13. Ma J, Xie G, Gao W, Yuan P, Qian L, Yu H, et al. Diode-pumped mode-locked femtosecond Tm:CLNGG disordered crystal laser. *Opt Lett.* (2012) **37**:1376–8. doi: 10.1364/OL.37.001376
14. Lagatsky A, Han X, Serrano M, Cascales C, Zaldo C, Calvez S, et al. Femtosecond (191 fs) $NaY(WO_4)_2$ Tm,Ho-codoped laser at 2060 nm. *Opt Lett.* (2010) **35**:3027–9. doi: 10.1364/OL.35.003027
15. Lagatsky AA, Koopmann P, Fuhrberg P, Huber G, Brown CTA, Sibbett W. Passively mode locked femtosecond $Tm:Sc_2O_3$ laser at 2.1 μm. *Opt Lett.* (2012) **37**:437–9. doi: 10.1364/OL.37.000437
16. Qin Z, Xie G, Kong L, Yuan P, Xu J. Diode-pumped passively mode-locked Tm:CaGdAlO4 laser at 2μm wavelength. *IEEE Photon J.* (2015) **7**:1–5. doi: 10.1109/JPHOT.2014.2381638
17. Kong LC, Qin Z, Xie G, Xu X, Xu J, Yuan P, et al. Dual-wavelength synchronous operation of a mode-locked 2-μm $Tm:CaYAlO_4$ laser. *Opt Lett.* (2015) **40**:356–8. doi: 10.1364/OL.40.000356
18. Schmidt A, Koopmann P, Huber G, Fuhrberg P, Choi SY, Yeom DI, et al. 175 fs Tm:Lu2O3 laser at 2.07 μm mode-locked using single-walled carbon nanotubes. *Opt Exp.* (2012) **20**:5313. doi: 10.1364/OE.20.005313
19. Pan Z, Wang Y, Zhao Y, Kowalczyk M, Sotor J, Yuan H, et al. Sub-80 fs mode-locked Tm,Ho-codoped disordered garnet crystal oscillator operating at 2081 nm. *Opt Lett*. (2018) **43**:5154. doi: 10.1364/OL.43.005154
20. Zhao Y, Wang Y, Chen W, Pan Z, Wang L, Dai X, et al. 67-fs pulse generation from a mode-locked Tm,Ho:CLNGG laser at 2083 nm. *Opt Exp*. (2019) **27**:1922. doi: 10.1364/OE.27.001922
21. Ma J, Qin Z, Xie G, Qian L, Tang D. Review of mid-infrared mode-locked laser sources in the 2.0μ m-3.5μm spectral region. *Appl Phys Rev*. (2019) **6**:021317. doi: 10.1063/1.5037274
22. Liu X, Popa D, Akhmediev N. Revealing the transition dynamics from Q-switching to mode locking in a soliton laser. *Phys Rev Lett.* (2019) **123**:093901. doi: 10.1103/PhysRevLett.123.093901
23. Liu X, Yao X, Cui Y. Real-time observation of the buildup of soliton molecules. *Phys Rev Lett.* (2018) **121**:023905. doi: 10.1103/PhysRevLett.121.023905
24. Liu X, Cui Y. Revealing the behavior of soliton buildup in a mode-locked laser. *Adv Photon.* (2019) **1**:016003. doi: 10.1117/1.AP.1.1.016003

Conflict of Interest: The authors declare that the research was conducted in the absence of any commercial or financial relationships that could be construed as a potential conflict of interest.